

Ba_{0.6}Sr_{0.4}TiO₃ Ferroelectric Fillers reinforced Poly(vinylidene fluoride)

Polymer Electrolytes for Dendrite-free Solid-state Li Metal Battery

Chen Yang^{a,b}, Hongjian Zhang^{a,b}, Mingtao Zhu^{a,b}, Ping Li^e, Hao Wu^{c,d*}, Qiushi Wang^{e*}, Yong Zhang^{a,b*}

a. State Key Laboratory of Advanced Technology for Materials Synthesis and Processing, School of Materials Science and Engineering, Wuhan University of Technology, Wuhan 430070, PR China. Email: zhangyong123@whut.edu.cn

b. Center for Smart Materials and Device Integration, Wuhan University of Technology, Wuhan 430070, PR China.

c. State Key Laboratory for Modification of Chemical Fibers and Polymer Materials, Donghua University, Shanghai 201620, PR China. Email: haowu@hbnu.edu.cn

d. Hubei Key Laboratory of Photovoltaic Materials and Devices, School of Materials Science and Engineering, Hubei Normal University, Huangshi, 435002, PR China.

e. Key Laboratory of New Energy and Rare Earth Resource Utilization of State Ethnic Affairs Commission, School of Physics and Materials Engineering, Dalian Minzu University, Dalian 116600, PR China. E-mail: wangqiushi@dlnu.edu.cn.

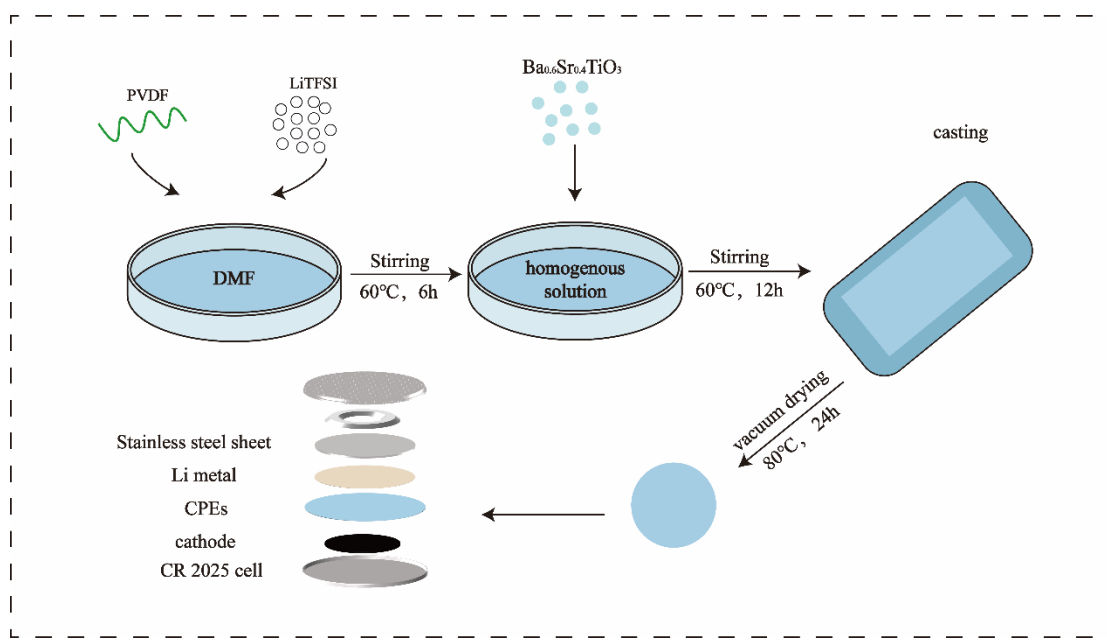


Figure S1. Schematic diagram of the preparation process for PVDF-4BST CPE.

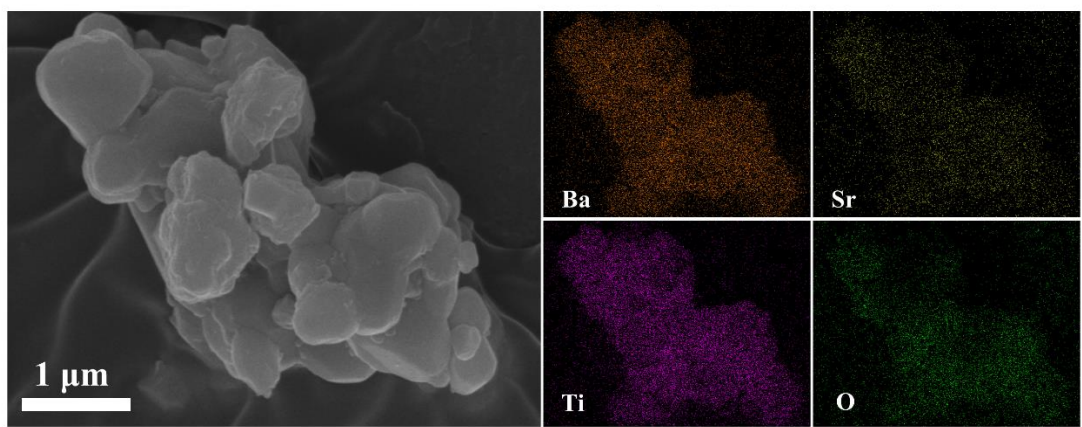


Figure S2. SEM and EDS mapping images of BST ceramic.

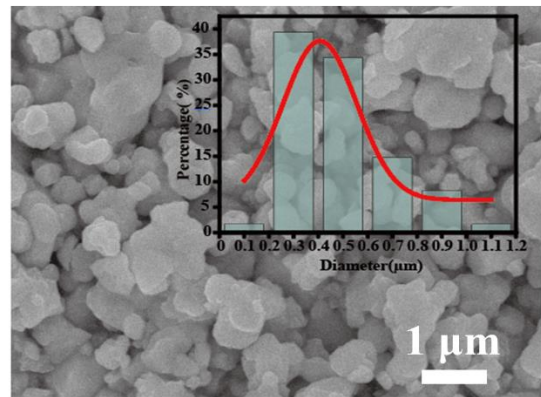


Figure S3. The size distribution of BST ceramic nanoparticles.

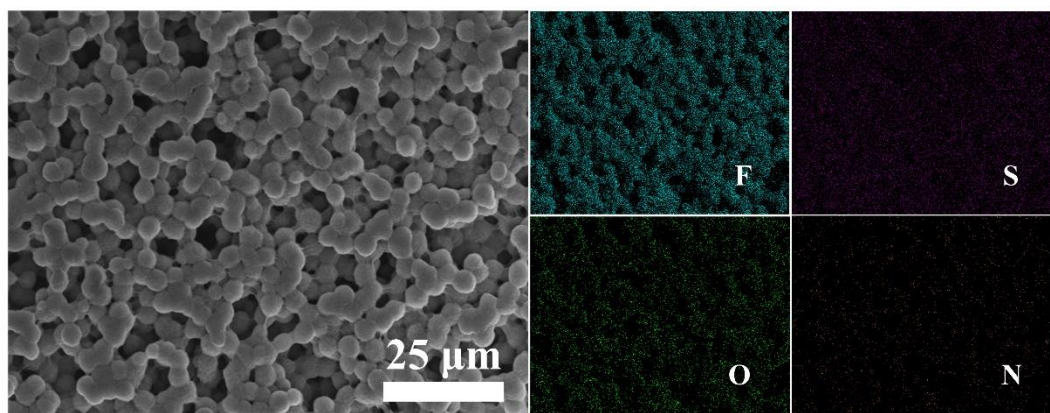


Figure S4. SEM image and EDS mapping of the PVDF SPE top surface .

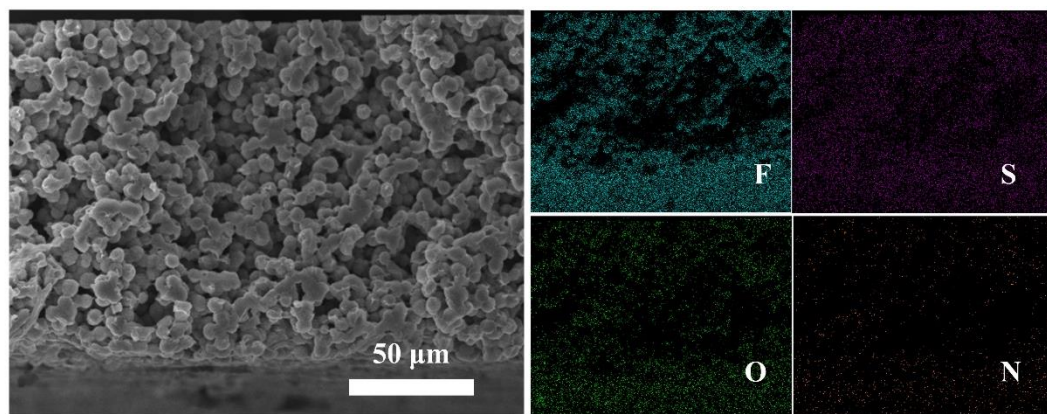


Figure S5. Cross-sectional SEM image and EDS mapping of PVDF SPE.

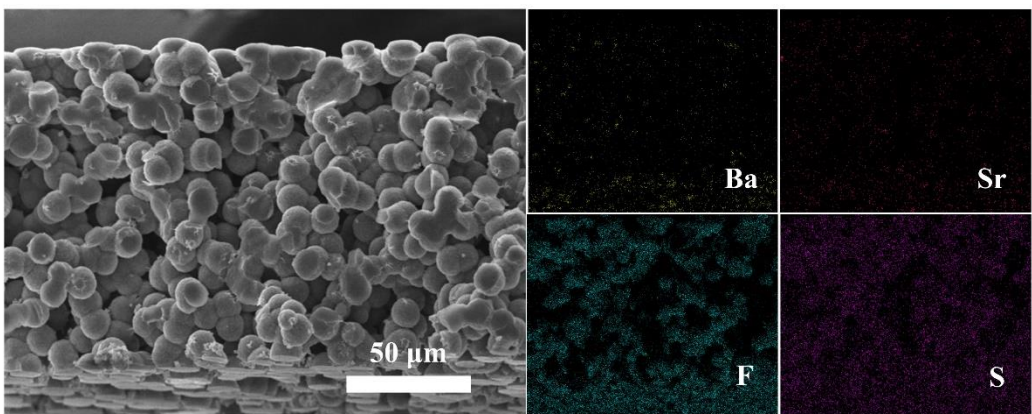


Figure S6. Cross-sectional SEM image and EDS mapping of PVDF-4BST SPE.

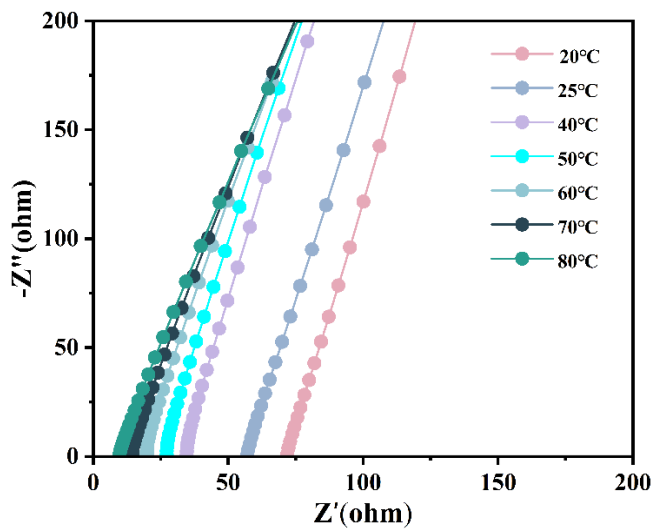


Figure S7. Electrochemical impedance spectra of PVDF CSEs with various temperatures.

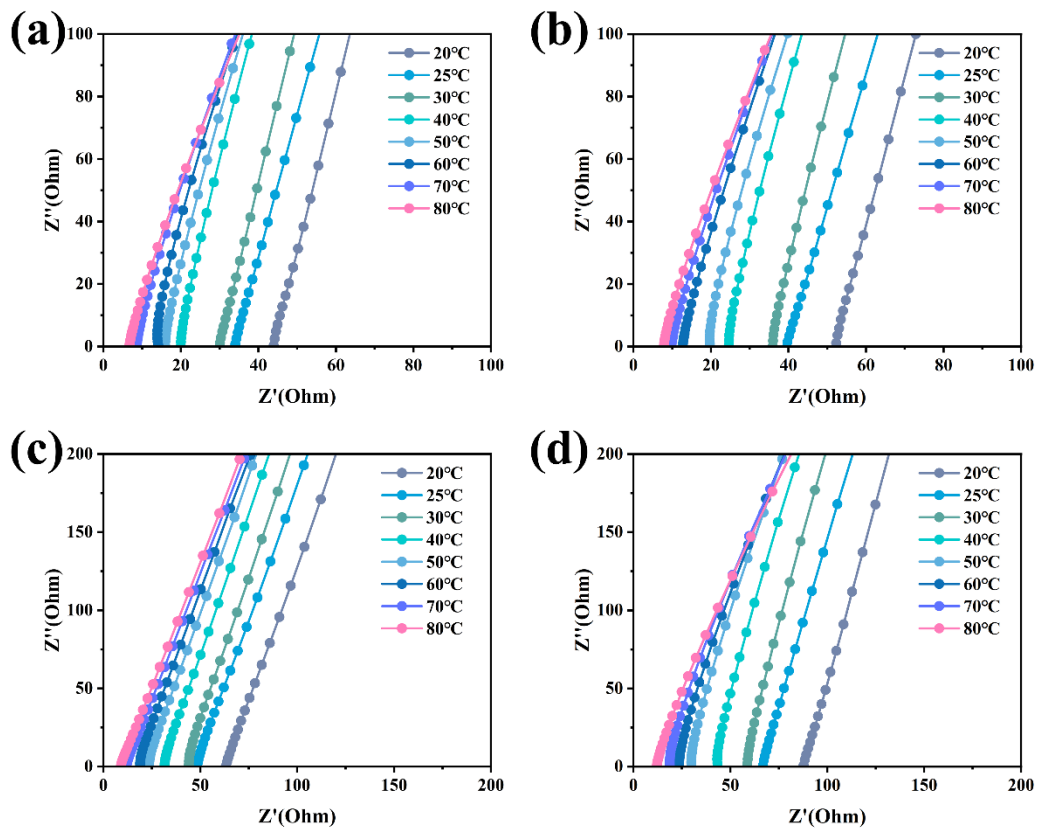


Figure S8. EIS plots of PVDF-xBST CPE from 20 °C to 80 °C ((a) $x=2$, (b) $x=6$, (c) $x=8$, (d) $x=10$).

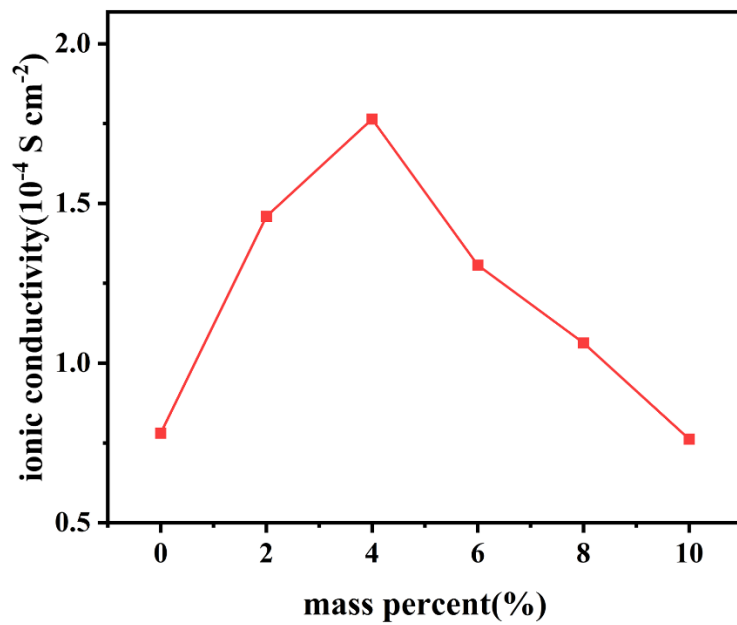


Figure S9. The ionic conductivity of PVDF-xBST CPEs at 25°C. ($x=0, 2, 4, 6, 8, 10$)

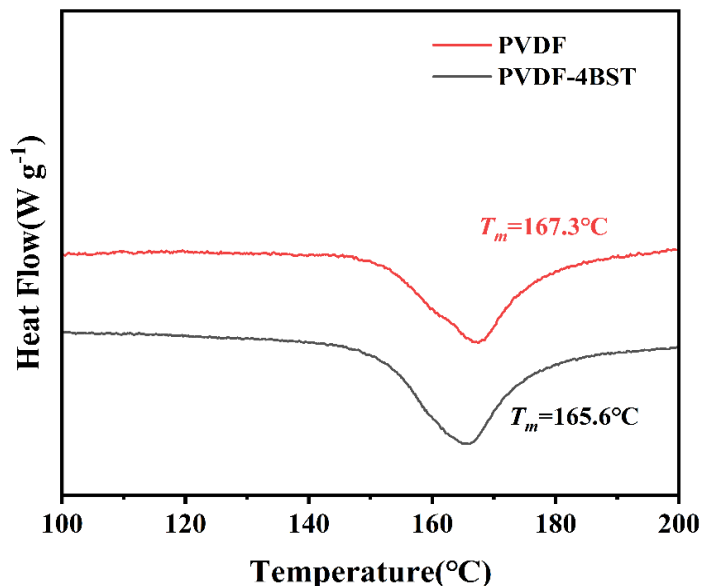


Figure S10. The Melting Temperature (T_m) of PVDF SPE and PVDF-4BST CPE.

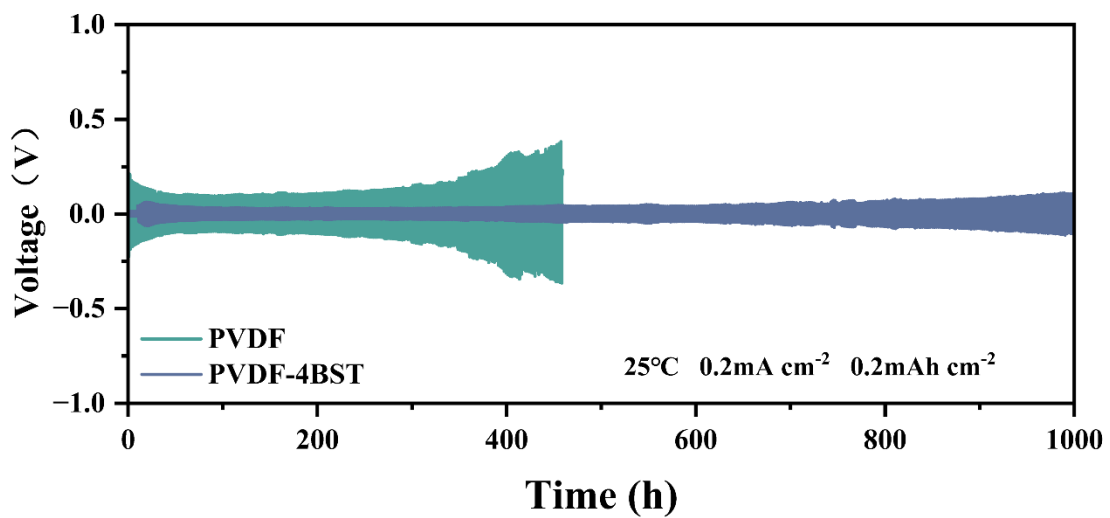


Figure S11. Galvanostatic cycles of Li|PVDF-4BST|Li and Li|PVDF|Li cells at 0.2 mA cm^{-1} .

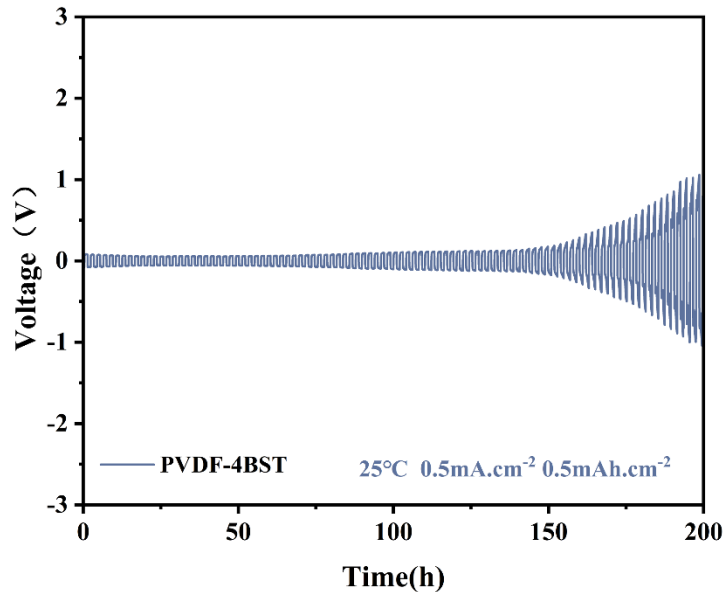


Figure S12. Galvanostatic cycles of Li|PVDF-4BST|Li cell at 0.5 mA cm^{-1} .

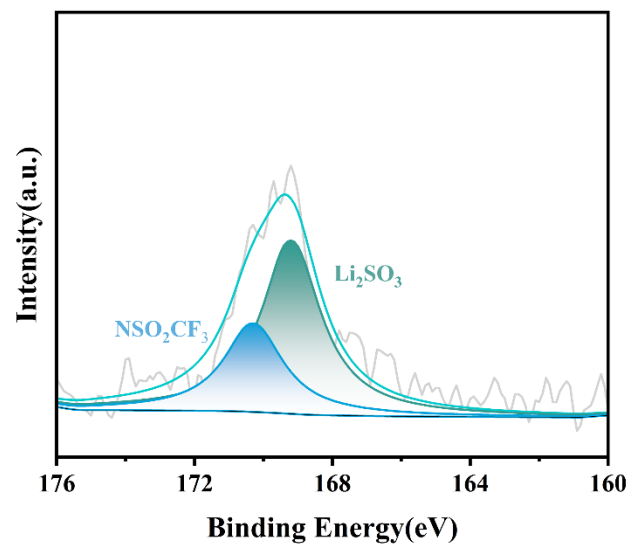


Figure S13. S 2p XPS spectra of cycled Li anodes from Li|PVDF|Li cell.

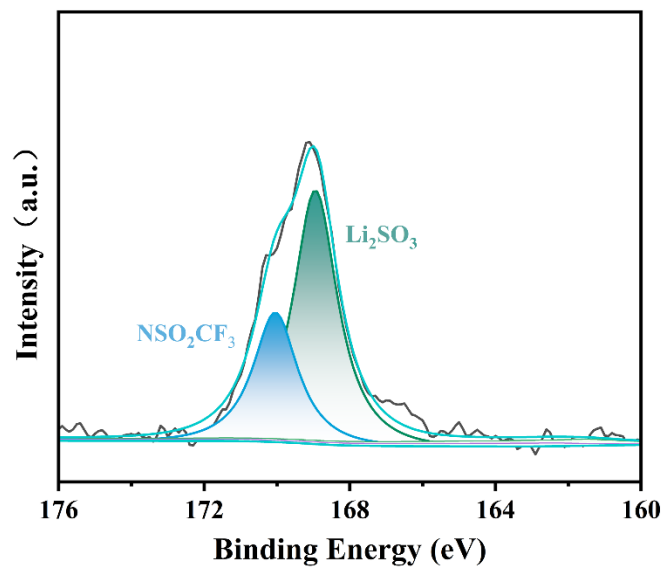


Figure S14. S 2p XPS spectra of cycled Li anodes from Li|PVDF-4BST|Li cell.

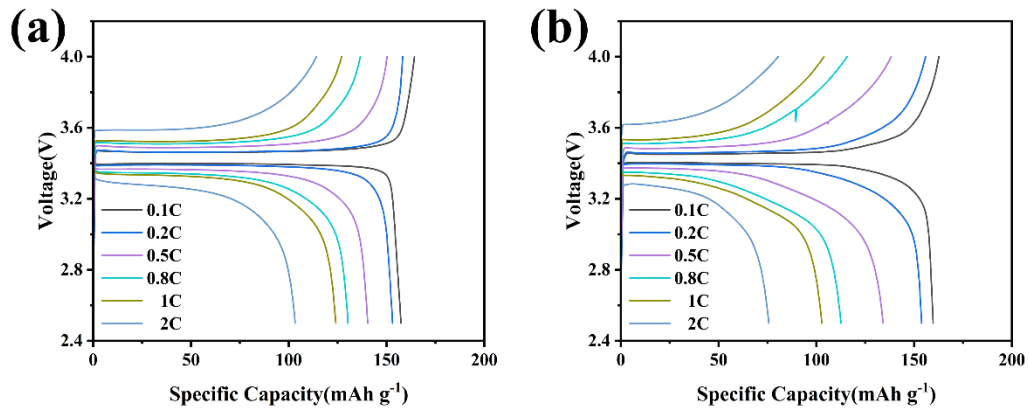


Figure S15. Charge/discharge curves of $\text{Li}|\text{PVDF}-\text{xBST}| \text{LiFePO}_4$ cells under different rates. ((a) $x=2$, (b) $x=6$)

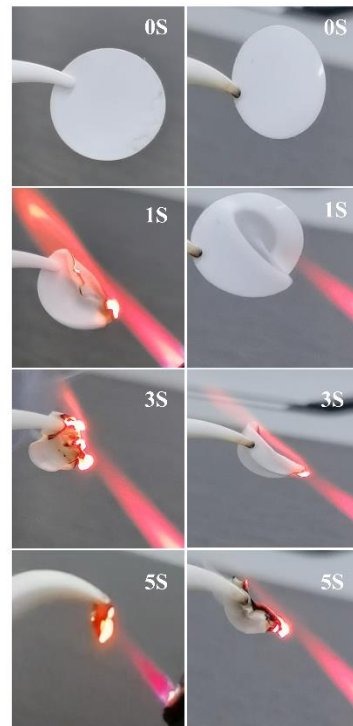


Figure S16. The combustion behavior of PVDF SPE (left) and PVDF-4BST CPE (right).

Table S1. The ion conductivity of PVDF -xBST CPE from 20°C to 80°C. (x=0, 2, 4, 6, 8, 10)

	20 °C	25 °C	30 °C	40 °C	50 °C	60 °C	70 °C	80 °C
0 wt%	5.69×10^{-5}	7.38×10^{-5}	8.16×10^{-5}	1.17×10^{-4}	1.49×10^{-4}	2.08×10^{-4}	2.84×10^{-4}	4.23×10^{-4}
2 wt%	9.29×10^{-5}	1.20×10^{-4}	1.37×10^{-4}	2.04×10^{-4}	2.56×10^{-4}	2.87×10^{-4}	4.75×10^{-4}	6.07×10^{-4}
4 wt%	1.24×10^{-4}	1.79×10^{-4}	2.15×10^{-4}	3.01×10^{-4}	3.57×10^{-4}	4.25×10^{-4}	6.74×10^{-4}	8.11×10^{-4}
6 wt%	8.80×10^{-5}	1.16×10^{-4}	1.28×10^{-4}	1.86×10^{-4}	2.32×10^{-4}	3.61×10^{-4}	4.69×10^{-4}	5.83×10^{-4}
8 wt%	7.26×10^{-5}	9.49×10^{-5}	1.04×10^{-4}	1.46×10^{-4}	1.95×10^{-4}	2.41×10^{-4}	3.84×10^{-4}	5.07×10^{-4}
10 wt%	5.24×10^{-5}	6.89×10^{-5}	7.81×10^{-5}	1.06×10^{-4}	1.53×10^{-4}	1.94×10^{-4}	2.43×10^{-4}	3.81×10^{-4}